Investigation of New Isotopes produced with a High-Intensity Uranium Beam in the Element Range from Hf to Np

J. Benlliure[1], P. Boutachkov[3], D. Cortina[1], T. Davinson[2], C. Domingo[3], F. Farinon[3], H. Geissel[3,4], J. Gerl[3], M. Gorska[3], H. Grawe[3], R. Janik[5], R. Kanungo[6], A. Kelic[3], B. Kindler[3], R. Knöbel[3], I. Kojouharov[3], T. Kubo[7], J. Kurcewicz[3], H. Lenske[4], J. Li[8], Y. Litvinov[3], B. Lommel[3], W. Long[8], G. Martinez-Pinedo[3], J. Meng[8], C. Nociforo[3], F. Naoki[7], T. Ohnishi[7], H.J. Ong[12], K. Otsuki[3], Z. Patyk[9], S. Pietri[3], B. Pfeiffer[3], M. Pfützner[10], W. Plaß[4], Zs. Podolyak[11], A. Prochazka[3], P. Regan[11], M.V. Ricciardi[3], C. Scheidenberger[3,4], H. Simon[3], B. Sitar[5], P. Spiller[3], J. Stadlmann[3], P. Strmen[5], B. Sun[3,8], H. Takeda[7], I. Tanihata[12], S. Terashima[7], B. Voss[3], H. Weick[3], J. Winfield[3], M. Winkler[3], H.-J. Wollersheim[3], Ph. Woods[2], S. Zhang[8]

1: Universidad de Santiago de Compostela, E-15706 Santiago de Compostela, Spain
2: University of Edinburgh, Mayfield Road, Edinburgh EH9 3JZ, United Kingdom
3: GSI, Planckstrasse 1, 64291 Darmstadt, Germany
4: Justus-Liebig University Giessen, Heinrich-Buff Ring 14-16, 35392 Giessen, Germany
5: Faculty of Mathematics and Physics, Comenius University, 84215 Bratislava, Slovakia
6: Astronomy and Physics Department, Saint Mary's University, Halifax, NS B3H 3C3, Canada
7: RIKEN Nishina Center, 2-1 Hirosawa, Wako, Japan
8: Beijing University, Joint Center for Nuclear Physics, Beijing, China
9: Soltan Institute for Nuclear Studies, Hoza 69, PL-00-681 Warsaw, Poland
10: Warsaw University, Instytut Fizyki Doswiadczalnej, Hoza 69, PL-00-681 Warsaw, Poland
11: Department of Physics, University of Surrey, Guildford GU27XH, UK
12: RCNP, Osaka University, 10-1 Mihogaoka, Ibaraki, Osaka 567-0047, Japan

Spokespersons: J. Kurcewicz, S. Pietri

Abstract:
The intensity of uranium projectiles which can be provided by the synchrotron SIS-18 has recently been increased to $2x10^9$/s and thus gives a worldwide unique potential to produce and investigate about 150 new neutron-rich isotopes with element numbers $72<Z<93$.

In the present proposal, at first we would like to extend the frontiers of known isotopes, study their production including nuclear charge-exchange reactions, i.e., measure the production cross sections.-- Secondly, implanting the new isotopes in a detector array will present the first half-live determination for these species. -- Thirdly, we want to measure one-proton- and one-neutron removal cross sections along with the corresponding momentum distributions of the (A-1) secondary fragment with the FRS as a high-resolution spectrometer. In addition, the charge-changing and interaction cross section will be measured to complement the differential measurements. From these data information on the neutron and proton radii can be deduced in a way which is presently well established for very light nuclides.

In this proposal the goals of our previous letter of intent have been focussed to the heavy projectile fragments (no fission products) and also the investigations with stored exotic nuclides is moved to a separate activity. The proposed measurements will be performed directly at the FRS using an advanced separation and identification scheme and an array of position-sensitive implantation detectors. The experiments will use new separation and detection techniques required for the development of the next-generation facility, the Super-FRS.

Motivation and Scientific Goals

In the mid 90's, FRS experiments set the scientific frontiers for medium mass neutron-rich isotopes [1]. In these experiments more than 120 new isotopes have been discovered, among them ^{78}Ni [2], and with these achievements a new research activity for fission studies was launched [3]. The applied physics program towards accelerator-driven reactors and nuclear-waste transmutation [4] has had its origin in these FRS experiments, too. Note, that the intensity at that time was a factor of more than 50 less compared what can be reached presently. Here, we want to study the heaviest projectile fragments created by a 1000 A·MeV ^{238}U projectile beam.

The presently proposed uranium experiment is driven by two main objectives: Firstly, exploiting the scientific possibilities in this research area of n-rich exotic nuclei with the high energies and intensities of the Uranium primary beam combined with the high-resolution performance of the FRS. Secondly, we have to explore new separation, identification and detection methods for increased primary-beam intensities up to the heaviest projectiles, a necessary step for the development of the future Super-FRS [5] at FAIR. The present SIS beams gradually approach FAIR intensities, a fact from which the ongoing experimental program can benefit. Moreover, the acceleration and extraction of SIS-beams at the space-charge limit is a challenge and practical experience needs to be gained with respect to extraction efficiency and stability. It is essential for a successful future that we gain now practical experience at the FRS.

The origin of heavy elements in the r-process is one of the outstanding problems in nuclear astrophysics [6]. Its understanding requires improved astrophysical modelling, stellar observations and nuclear physics data, like masses (Q-values) and half-lives.

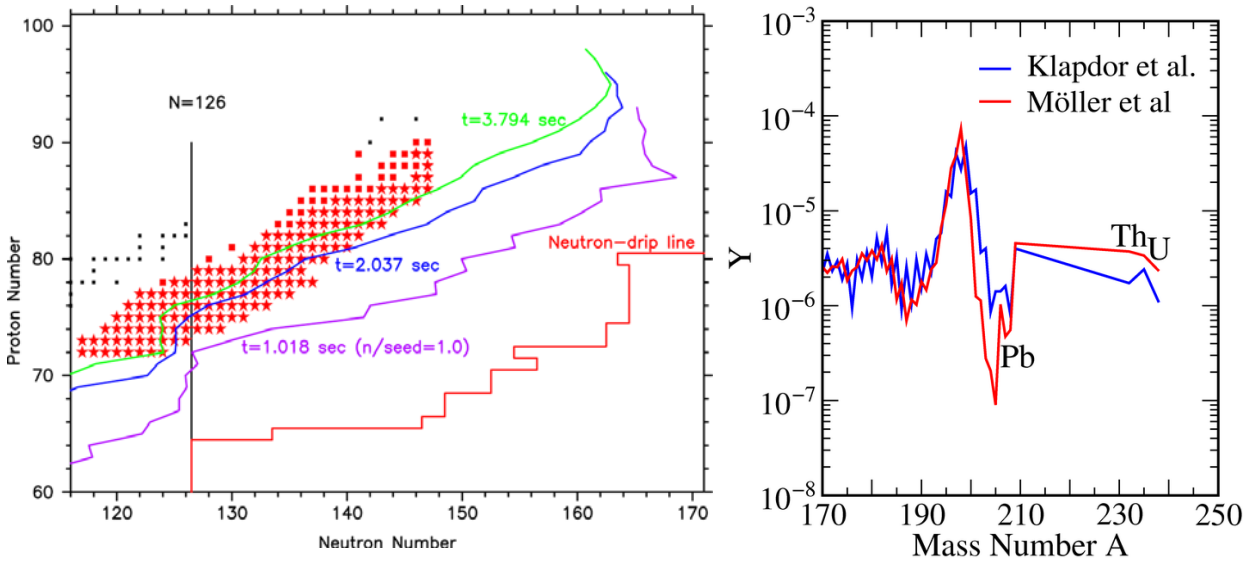

Fig. 1: The left panel shows the evolution of the r-process path. The line n/seed = 1 corresponds to the freeze-out of neutron captures. At later times a competition between neutron captures and beta decays takes place as the r-process material decays to stability. During this phase the nucleosynthesis path proceeds along the region that will be explored in the present proposal (red stars). The right panel shows the impact that changes in the beta decay half-lives have in the final r-process abundances for nuclei with A>170.

Currently, there are several stars for which abundances of the cosmochronometers Uranium and Thorium [7] have been observed. For some of them, there are also Lead observations. The abundances of Uranium and Thorium can be used to determine the age of our galaxy. For that it is necessary to determine their initial abundances which have to be obtained from theoretical r-process calculations. These calculations should additionally reproduce the observed Lead abundances. The

structure and half-lives of elements in the r-process path between Gold and the actinides play an important role in determining the final yields of Lead, Uranium and Thorium. The left panel of figure 1 shows the r-process path at different times, a calculation based on the model of ref.[8]. To estimate the impact that beta decay half-lives have in the final abundances of Lead, Uranium and Thorium, we have performed two calculations using the half-lives of refs.[9] and [10] (right panel). Changing from one set of half-lives to the other results in a change of the ratio of Uranium to Thorium abundance of log(U/Th) = 0.164 that translates in a age difference of 3.55 Gyr.

A further clear motivation for the present proposal is demonstrated from previous FRS-ESR experiments [19], see also LoI44. We have demonstrated along with new mass measurements the discovery of n-rich isotopes below uranium with an effective intensity of a factor of 100 lower compared to the goals of the present proposal. From this it is obvious that the search for and investigation of new isotopes directly at the FRS has a high discovery potential.

Besides the astrophysical motivation, there are also nuclear structure and reaction interests. The production reactions will be studied by cross section and primary momentum measurements. These data and especially the measured rates will be a realistic base for planning detailed spectroscopy of proceeding experiments. Projectile fragmentation at the FRS has proven to be an ideal experimental tool for these survey studies. The second physical goal is half-live measurements for nuclides beyond the N=126 shell, close to the calculated r-process path, see figure 1 and table 2. (Directly at the shell closure Z=82 and N=126 (^{202}Os, ^{203}Ir, ^{205}Au) there are approved experiments for detailed gamma and decay spectroscopy including states with high angular momentum [11].) Combined with the search for new isotopes and half-life and reaction studies we want to measure the proton and neutron removal cross sections and the momentum distributions for the corresponding (A-1) secondary fragments. The determination of the charge-changing and interaction cross sections will complement these differential measurements. These investigations will yield information on both the proton and neutron density distributions. This will be the first time that these techniques will be employed for heavy elements which is experimentally a great challenge due to the required momentum resolution and the atomic energy straggling and charge-state populations [12,13]. Mapping the nuclear density distribution via precise momentum measurements is well established for light dripline nuclei [14-18].

Experiment

1. Production of new neutron-rich isotopes

The first experimental goal is to produce and identify new neutron-rich isotopes in the element range between Hafnium and Neptunium. For this a 1000 A·MeV $^{238}U^{73+}$ primary beam will be extracted from the synchrotron SIS-18 and focussed on the production target placed at the entrance of the FRS. In general we plan to use a Be target of optimum thickness. In addition we will explore also the rates with a medium Z target (Cu) to get higher excitations of the prefragments. The expected maximum intensity for the primary beam will be more than $2 \cdot 10^9$ /s. A principal problem for a realistic rate calculation for the new isotopes is that the cross sections are only measured close to the valley of stability. Therefore, the first physical measurements will be the experimental determination of the production cross sections and the achievable optimum rates. Presently, we take extrapolated cross sections calculated by the computer codes EPAX [20], ABRABLA [21], and COFRA [22], in general the codes have the information from previous experimental data implemented. In this way, previous FRS experiments have contributed to the present realistic predictions. The transmission and the losses due to the inevitable atomic charge-state population are taken into account from realistic ion-optical simulations employing the Monte Carlo code MOCADI [23] and the transport code LISE [24]. The experimental set at the FRS is schematically presented in fig. 2. Layers of matter have been placed at the different focal planes to achieve spatial separation of the fragments of interest. They have to be efficiently separated from the primary beam and the undesired fragments produced with higher rates. The atomic charge-state population of the

primary beam is really an experimental problem which requires suitable layers of matter to apply the separation scheme of energy-loss and magnetic rigidity analysis (Bρ-ΔE-Bρ) combined with energy deposition measurements in ionization chambers (IC) and time of flight (ToF), i.e. the Bρ-ΔE-ToF technique. The key to unambiguous separation and identification in flight, in spite of the atomic charge states, is tracking to identify those ions that experience charge changing and to apply the highest projectile energies ($B\rho_{max}$=18 Tm) which is unique for GSI. The Bρ measurements will be performed by accurate position measurements using high-rate time projection chambers (TPC). The primary beam intensity will be measured with a secondary electron monitor. The particle identification will be supported by isomer tagging of known isotopes at the final focal plane.

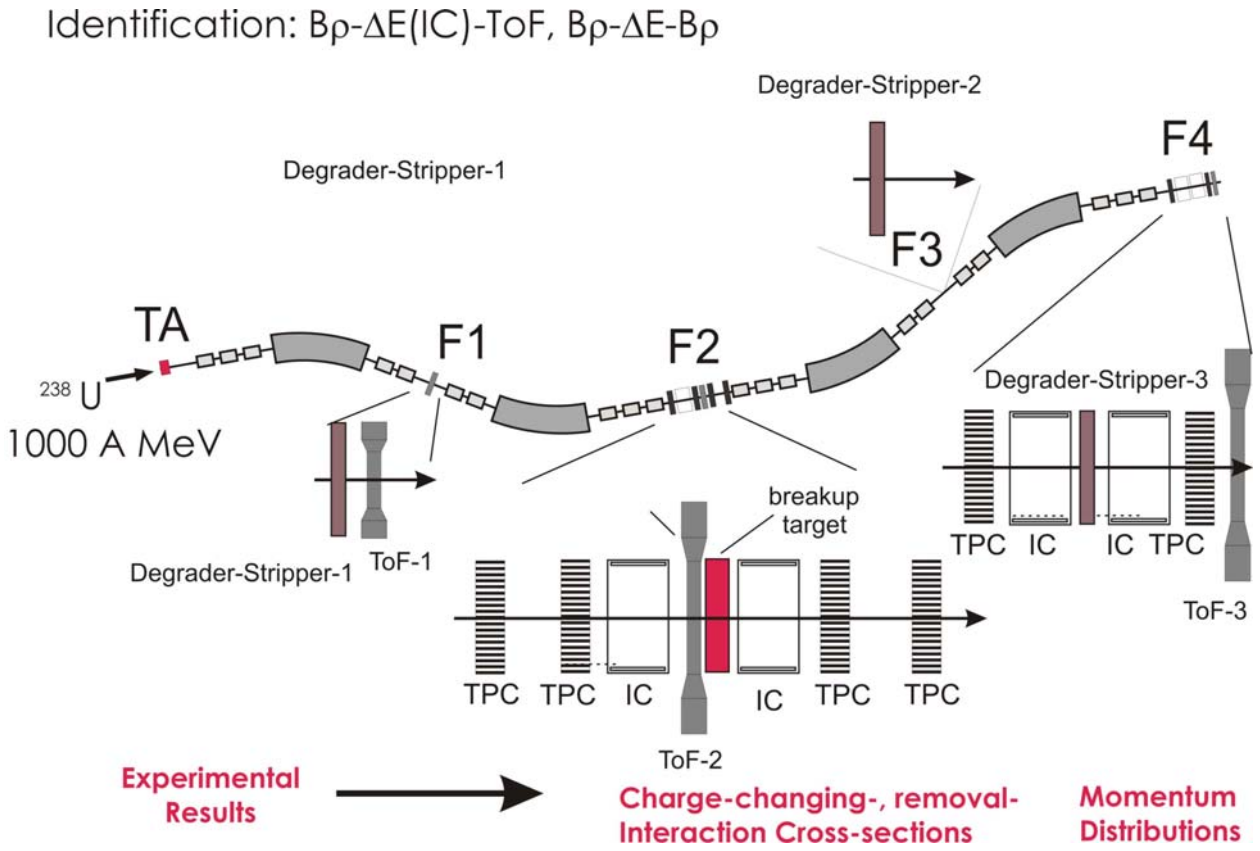

Fig. 2: Experimental setup for the identification and investigation of new neutron-rich isotopes in the element range from Hf to Np. The function of the detector systems and the use of the FRS as high-resolution spectrometer are described in the text.

The range of isotopes aimed for the present exploratory search reaches from neutron-rich Hf isotopes up to Np. The rates have been calculated using the codes LISE and MOCADI where specially extrapolated cross sections have been implemented. The isotopes which can be observed for the first time are indicated in fig. 3. 148 isotopes can be observed for the first time with mainly three field settings of the FRS. The lower limit has been assigned to a rate of 10^{-5} /s which means about 1 ion per day. It is planned to run each setting for 3 days. The in-flight particle identification starts with the detector system at the central focal plane F2 during the isotope search run. For these series of measurements it is not required to operate ionization chambers at F2, whereas the TPC will measure the momentum distribution of the primary fragments emerging from the target. The F1 degrader-stripper system is tuned to have a manageable rate for the F2 detectors. In the runs for new isotope search a variable achromatic degrader system will be applied to achieve the spatial separation at F4 where two IC are employed with a suitable stripper medium in between to unambiguously disentangle the different ionic charge-states and elements.

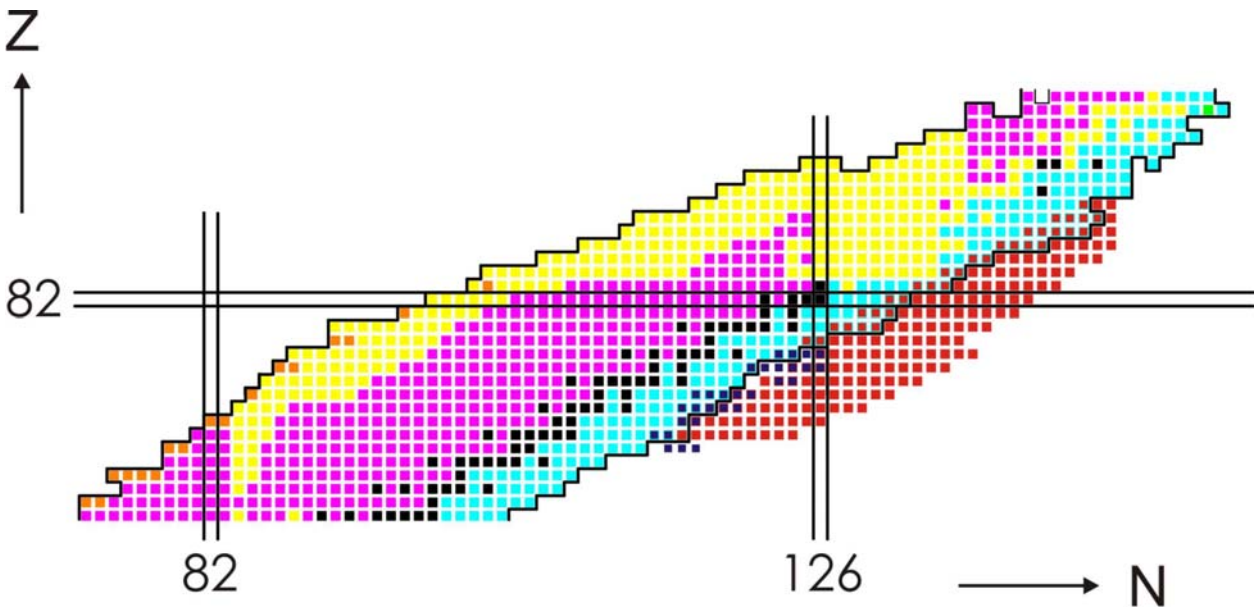

Fig. 3: Part of the chart of nuclides indicating the interest of the present proposal. The isotopes of interest are indicated by crimson colour. The dark blue squares represent new isotopes of a previous FRS experiment where also half-life measurements have been performed for Lead fragments [25]. The search for the new isotopes will be done by mainly three different field settings of the FRS, see Table 1.

Z	Last known	Accessible Nuclides		Rate (s^{-1})		FRS-Setting Reference Fragment	New Nuclides
		From	To	From	To		
72	^{188}Hf	^{188}Hf	^{196}Hf	2.2E-03	1.6E-05	^{204}Os	8
73	^{189}Ta	^{189}Ta	^{199}Ta	2.9E-03	2.0E-05		10
74	^{192}W	^{192}W	^{203}W	3.6E-03	1.3E-05		11
75	^{194}Re	^{195}Re	^{206}Re	6.5E-03	1.9E-05		12
76	^{196}Os	^{198}Os	^{209}Os	6.7E-03	2.7E-05		12
77	^{198}Ir	^{201}Ir	^{212}Ir	8.0E-03	2.3E-05		12
78	^{202}Pt	^{204}Pt	^{215}Pt	1.0E-02	1.2E-05		12
79	^{205}Au	^{204}Au	^{215}Au	4.8E-01	1.0E-03	^{212}Hg	10
80	^{210}Hg	^{207}Hg	^{218}Hg	7.0E-01	1.3E-04		8
81	^{212}Tl	^{210}Tl	^{221}Tl	6.1E-01	8.3E-04		9
82	^{214}Pb	^{213}Pb	^{223}Pb	1.4E+00	1.0E-04		9
83	^{218}Bi	^{216}Bi	^{226}Bi	6.2E-01	1.0E-05		8
84	^{220}Po	^{219}Po	^{228}Po	1.4E+00	2.2E-04		8
85	^{223}At	^{222}At	^{231}At	1.4E+01	7.2E-05	^{226}At	8
86	^{228}Rn	^{225}Rn	^{233}Rn	3.8E+01	2.3E-04		5
87	^{232}Fr	^{228}Fr	^{234}Fr	1.0E+02	1.8E-02		2
88	^{234}Ra	^{231}Ra	^{235}Ra	9.5E+01	5.3E-01		1
89	^{234}Ac	^{234}Ac	^{236}Ac	2.3E+02	1.1E+01		2
91	^{239}Pa						
					Sum:		144

Table 1: Calculated rates for the accessible new isotopes produced with $2{\cdot}10^9$ ^{238}U projectiles/s in a 2.5 g/cm^2 Be target equipped with a 220 mg/cm^2 Nb post-stripper. The rates include a full transmission calculation and the ionic charge-state population. The layers of matter in the different focal planes are selected to achieve mainly isotopes of the element range of interest.

Beamtime request for new isotope search:
To cover the calculated range of new isotopes with a lower limit for the rate of 10^{-5} /s which means about 1 ion per day. It is planned to run the 3 settings (see Table1) each setting for 3 days.
(**sum = 9 days)**

2. Half-life Measurements

A strong motivation for half-life experiments in unknown territory of nuclides is that present theoretical models are in general not in good agreement with the experimental data far from the valley of stability as illustrated with results from a previous FRS experiment [25]. An influence of these uncertainties in the knowledge of lifetimes is discussed in the context of astrophysical relevance above. Note, in the region between N>128 and Z<82 we come very close to the r-process path.

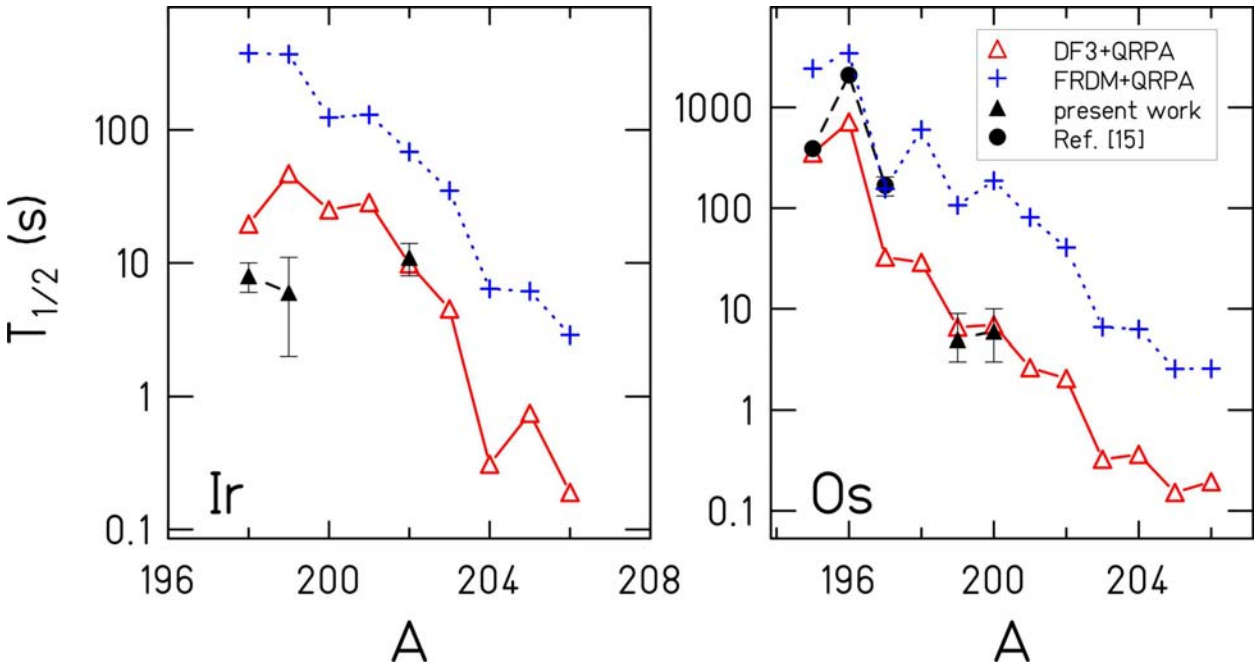

Fig. 4: Results from a recent FRS experiment [25] clearly demonstrate the need of experimental data to guide the theoretical model predictions. The total β-decay half-lives for Ir and Os isotopic chains calculated with different theoretical approaches (DF3+CQRPA [26], FRDM [27]) compared with experimental values from Ref [25].

The experimental setup from previous RISING experiments or the new one with the AIDA implantation array at the final focal plane, F4, of the FRS are both suited for the proposed decay experiments of implanted atoms. It consists of two TPC position detectors, two consecutive IC detectors for charge measurement and a fast plastic detector for ToF. The detectors enable a unique ion-by-ion determination of charge, mass, energy, direction and focal plane position of the beam species selected by the FRS.

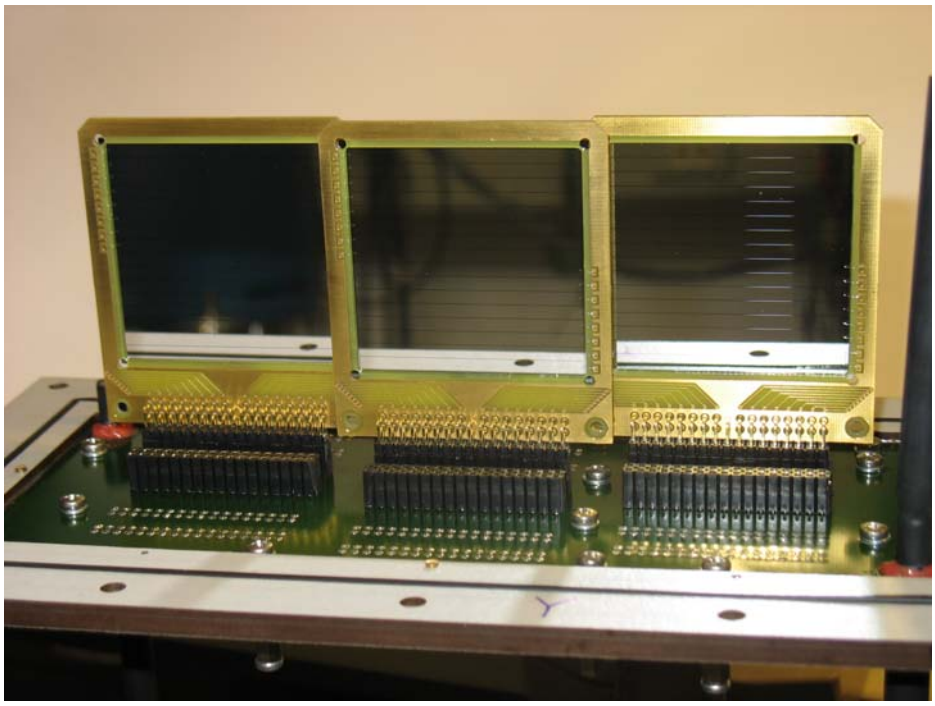

Fig. 3: The 'active catcher' of the present RISING campaigns consists of three Si strip detectors.

A variable homogeneous degrader behind these particle identification detectors slows down the ions before implantation into the active catcher of RISING. This device incorporates two layers of three DSSSD covering fully the focal plane. The catcher allows the detection of both the implantation signal of a heavy isotope and the subsequent signal of the β-particle from its the decay. The typical β-detection probability is larger than 80%. The 16x16x3 = 768 pixels of the detector enable an increased rate of implanted nuclides without losing the correlation between identification in-flight and the beta-decay. For a recent experiment on lifetimes of Lead fragments a method based on statistical correlations including the spill structure of the beam and the unknown lifetime as free parameter has been developed and applied successfully [28]. As a consequence the lifetime may even exceed the cycle time of the accelerator (about a few seconds) and nuclei with lifetimes up to 30 s can be investigated. Shorter lifetimes down to 10 ms are also possible due to the segmentation and a logarithmic amplifier which enable that betas can be detected while heavy ions pass through other strips.

The background from implanted ions and their decay products up to a nucleus with lifetime longer than the run time will increase in the detector during the experiment. However, by a suitable selection in the FRS and in addition by the good separation in range with the monoenergetic degrader this background activity can be reduced. The total background rate coming mainly from nuclides with lifetimes longer than the cycle time but much shorter than the duration of the experiment will then be at an equilibrium and in good approximation the background decay rate will equal the rate of implanted ions times the length of the decay chain up to long-lived nuclei (τ >length of experiment). The fraction of random coincidences can then be calculated from Poisson statistics. For example, with an extraction time of 1s and an inter-spill time of 4 s a rate of 20 implanted ions per spill around ^{223}Po will only lead to a fraction of random coincidences of about 10 % which can be handled in the statistical analysis. This already takes into account the long decay chains including alpha emitters for this case.

A system where the catcher is exchanged frequently could have some advantages but it would require a rather thick catcher of about 1mm thickness and this would consume a lot of material. More important is the advantage given by the granularity of the detector together with the individual identification of the ions. With such an 'active catcher' we can run at even higher rates than with a passive catcher which is exchanged after each spill. Lifetimes shorter than one second will be measured during the spill.

We will go beyond N=126 and concentrate on lifetime measurements only which complement the approved FRS-proposal aimed at the investigation of high-spin isomers at the N=126 line [11]. A first setting will concentrate on ^{208}Au (reference fragment centred at the optical axis). As always in the course of these lifetime measurements, only a few nuclei around the reference fragment can be implanted thus we will have to change the FRS setting to implant other nuclides. With an intensity of $5x10^{9}$ ^{238}U per spill and an enlarged cycle time of 5 s ^{208}Au fragments can be implanted at an average rate of 0.026 ions/s with good separation to keep the total rate in this setting even below 1 ion/s, see Table 2. After accumulating decays over 1 day and considering the efficiency of the detectors, 749 decays should be observed. This amount should stick out clearly from the background of random coincidences. But with less than 100 per day this condition is not given for an activated detector. Several setting in the region of N>126, Z<82 are planned to cover the whole area. Afterwards the area around ^{223}Po will be investigated. The count rates for a ^{223}Po setting are given in Table 2.

Table 2: Two examples of rates of implanted nuclei and expected identified decay events. In addition four more settings are planned for half-live measurements.

Table 2

^{208}Au setting	Implantation rate /s	Decay events /day
^{206}Pt	1.4E-03	40
^{207}Pt	1.0E-03	30
^{206}Au	8.2E-03	236
^{207}Au	6.2E-02	1794
^{208}Au	2.6E-02	749
^{209}Au	6.7E-03	193
^{208}Hg	2.4E-02	691
^{209}Hg	1.1E-01	3053
^{210}Hg	8.4E-02	2419
^{211}Hg	8.0E-03	230
^{210}Tl	8.0E-04	23
^{211}Tl	1.9E-02	547
sum	0.35	

^{223}Po setting	Implantation rate /s	Decay events /day
^{219}Bi	5.5E-03	158
^{220}Bi	5.4E-02	1544
^{221}Bi	3.5E-02	1020
^{222}Bi	3.2E-03	92
^{221}Po	7.6E-02	2177
^{222}Po	5.0E-01	14400
^{223}Po	2.2E-01	6293
^{224}Po	4.7E-02	1354
^{225}Po	1.0E-03	30
^{223}At	1.2E-02	333
^{224}At	4.9E-01	13968
^{225}At	8.9E-01	25661
^{226}At	1.4E-01	3974
^{227}At	1.2E-03	34
^{226}Rn	6.9E-03	199
sum	2.5	

The whole range of nuclides with unknown lifetimes we want to cover in this experiment can be reached in the following 6 settings centred at ^{239}Rn, ^{223}Po, ^{216}Pb, ^{211}Hg, ^{208}Au, and ^{205}Pt fragments. We must consider that each setting is optimized for only a few nuclides in order to achieve the good separation. One of the key points is the separation in atomic range with a monoenergetic degrader in contrary to the search for new isotopes with the achromatic degrader. As we have to slow down the ions the suppression of atomic charge states, which may influence the particle identification, will not be as good as at high energies but these nuclides have a substantially longer half-live.

Beamtime Request for Half-live Measurements:

The whole range of nuclides with unknown lifetimes we want to cover in this experiment can be reached in the following 6 settings centred at ^{239}Rn, ^{223}Po, ^{216}Pb, ^{211}Hg, ^{208}Au, and ^{205}Pt fragments. One setting should run for one day. In addition for each setting 4 hours are required to tune the atomic range and to optimize the separation.

In total we request: 1 week

3. Momentum distributions of secondary fragments after one-nucleon removal reactions

The proton and neutron density distributions are basic ground-state properties of each nuclide. The charge radii of stable heavy ions have been determined by classical electron scattering [29], by analysis of atomic transitions in exotic atoms orbited by negative particle much heavier than electrons (e.g. muons, antiprotons) [30], or by laser spectroscopy of the hyperfine structure and isotope shifts [31]. The information is strongly restricted by the isotopes which could be provided by the applied production and separation scenario of the target nuclei or reaction products. Presently, only laser spectroscopy, analyzing the isotope shift and hyperfine structure of spectral lines, yields access to charge radii of short-lived nuclides. Experimental information on both matter distributions of heavy nuclei over a large Z range of stable isotopes have been deduced from annihilation measurements of antiprotonic atoms [32, 33]. This method gave reliable results as demonstrated for nuclei which have been studied with other methods as well. Again the limitation was the availability of targets and thus only stable and long-lived target material could be applied in the antiprotonic method. In addition the material had to be selected such that the (A-1) product after the annihilation could be quantitatively analysed by radiochemical methods.

Here, we propose a novel and quite versatile method for very heavy ions namely to measure the momentum distributions of fragments after one proton or one neutron have been removed from the selected primary fragment in addition to the interaction and charge-changing cross sections.

Concerning the physics case, the proposed experimental studies will provide novel insight into the evolution of the mass distribution in heavy nuclei by varying the charge-mass asymmetry. Measurements of momentum distributions are a standard tool of reaction physics for light exotic nuclei, e.g. [34, 35]. However, in the mass region A~200 considered here one encounters new challenges by the much higher density of states in the proton and neutron valence shells, see fig. 6. This is already true on the mean-field level, not to mention the additional effects resulting from core polarization. Removal reactions on heavy nuclei will therefore correspond to an average over breakup cross sections from states of an energy window below the lowest particle emission threshold. Hence, breakup reactions can be expected to be especially sensitive to the skin components of nuclear density distributions. Measuring proton and neutron removal cross sections on the same isotopes will allow the independent investigation of the evolution of the proton and the neutron valence components along isotopic chains.

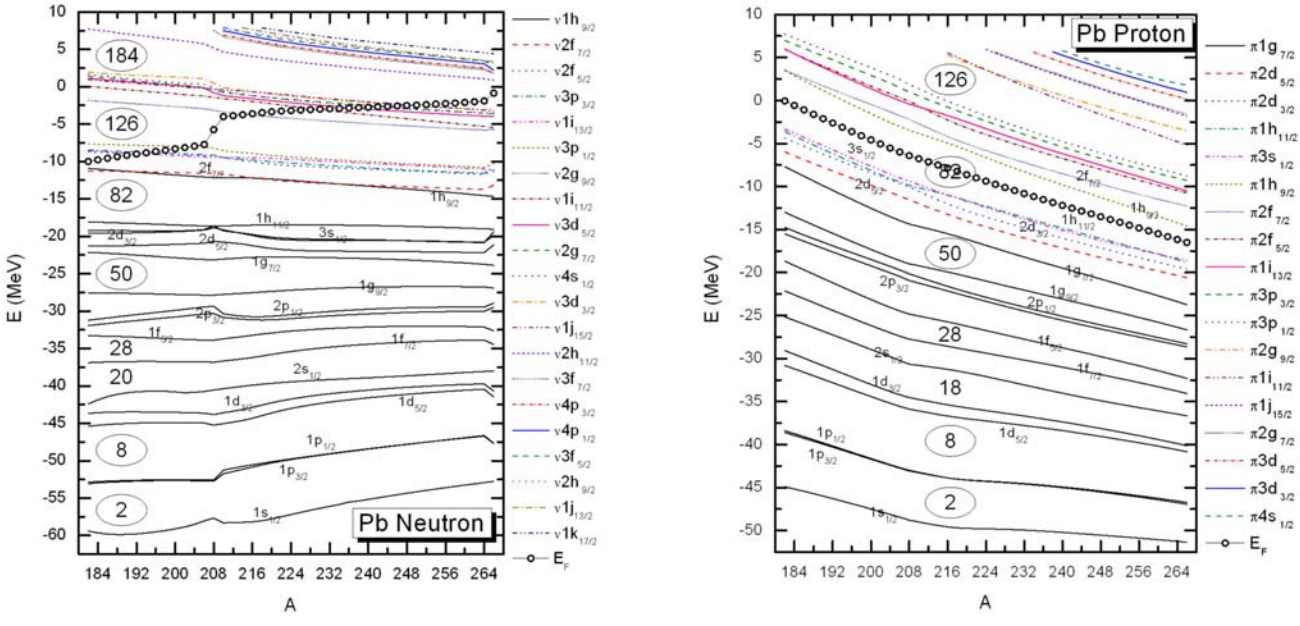

Fig. 6: Calculated neutron and proton single particle energies for Lead isotopes [36]. The Fermi levels are indicated by open circles.

Such results will provide important constraints on nuclear models: A prediction of any type of self-consistent HFB calculations is that both proton and neutron rms radii increase with increasing neutron excess, but the proton radii with a milder variation. This behaviour is directly related to the action of the isovector mean-field potential, e.g. as seen in Fig. 7 below. Therefore, precise results on the isotopic dependence of proton and neutron valence rms radii will provide additional constraints on the isovector potential and, as such, on the symmetry energy coefficient of mass formulas and microscopic model.

A second, equally exciting option of the experiment is to exploit the strong absorption for spectroscopic work. Scattering of heavy nuclei on nuclear targets is a strongly absorptive reaction. In that respect, these systems behave similar to antiproton-ion scattering, although the physical processes behind the large reaction cross section are very different, but as seen from ref. [37] what counts is only the overall strength of the flux going into the non-elastic channels.. Hence, similar to the antiproton case investigates theoretically in ref. [37] measurements of total reaction cross sections will provide independent information on the rms-radii., In ref. [37] it was shown that at high energies around 1 A·GeV the absorption cross sections are directly proportional to the rms radii of the reacting nuclei. Within the eikonal approximation the proportionality constant is even obtained analytically. It is found to depend only on the incident energy besides numerical constants, meaning that it acts a mass-independent scaling factor. Therefore, it is easily determined experimentally from measurements on stable isotopes with known values of the corresponding rms radii.

The need for experimental data on the nuclear matter distribution is demonstrated by radii calculations using HFB and RMF microscopic calculations employing different effective forces. The deviations of the theories are especially large for the neutron predictions.

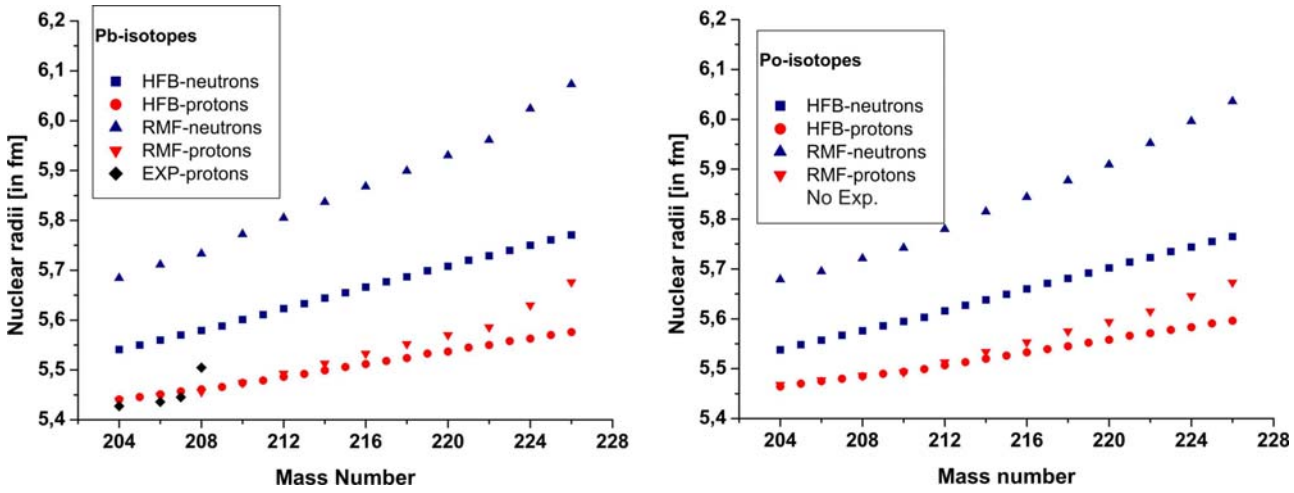

Fig. 7: Calculated and measured nuclear radii for Pb and Po isotopes. Only for a few Pb isotopes the charge radii have been measured [40]. Almost no experimental information is available for the neutron density distributions. The calculated neutron and proton radii predicted within the Hartree-Fock-Bogolyubov (HFB)[38,39] and the Relativistic Mean Field (RMF)[41] methods are presented.

Experimental details in addition to the setup discussed above:
Practically, this means, we fully identify a selected fragment in flight up to central focal plane of the FRS where the isotope of interest impinges on a hydrogen (polyethylene) break-up target. Either a radiation resistive ToF detector like a Diamond system will be positioned at the focal plane at F1 or a Cherenkov counter placed at F2 will be used to measure the velocity in front of the breakup target. In the first measurement cycle one proton is removed in the next a neutron is removed from the same incident fragment in a collision at about 900 A·MeV. The measured momentum distributions will reflect the nuclear orbitals of the removed nucleons. These high-resolution momentum measurements include the determination of the corresponding removal cross section. Complementary to this set of differential data we will measure also the charge-changing and the interaction cross sections. The determination of the nuclear charge-changing cross section will be performed with the isotopically separated fragment beam penetrating two ionisation chambers (IC) with the interaction target in between. Due to the inevitable atomic charge-state population of the fragments penetrating matter (target, degraders, detectors) the challenge is to correct this influence.
A simulation demonstrating the feasibility is presented in fig. 8 for an example of nucleon removals off ^{233}U fragments. From the simulations we can conclude that we can realize the goal of accurately measuring the 5 physical quantities (2 removal cross sections, the interaction and charge-changing x-sections and the corresponding momentum distribution) for one isotope. Since this part of the proposal requires the highest experimental challenges we plan to start this with the ^{238}U ions and neighbouring isotopes. Special dimensions (stripes, holes) of the production target will be employed similar as we have performed our experiments with pionic atoms [42]. Since the nuclear charge (proton radii) distribution of ^{238}U is experimentally known this measurement will serve as a bench mark. It is important to measure the evolution of the matter distribution. The main goal is to deduce information on the neutron skin which would present important constraints on the effective interactions in nuclear models.

This measurement will be worldwide unique and requires the highest performance of the FRS and the detector systems including tracking. After this pioneering test measurement we plan to measure n-rich short-lived isotope chains which could not been studied with the restricted experimental methods up to now. Note, our novel method is versatile and can be applied to all nuclides with count rates above 10 s^{-1}.

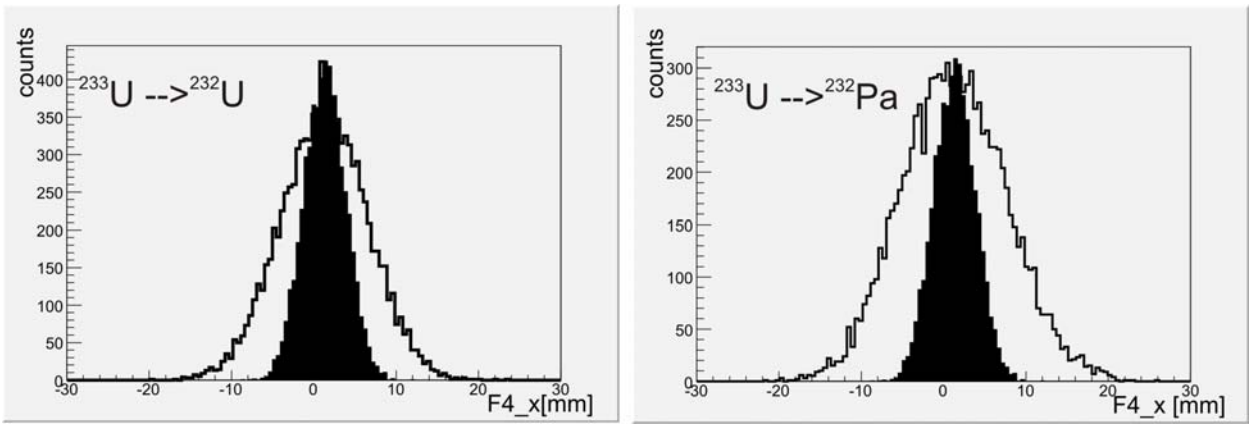

Fig. 8: Calculated position distributions at the final focal plane for neutron (left panel) and proton removal (right panel). A 1 g/cm^2 Al degrader at F1 and a breakup target also of 1 g/cm^2 has been considered in this simulations. The resolution function of the FRS is indicated by the full histograms. The ion-optical dispersion and the magnification were 7.22 cm/% and 1.11, respectively.

Beamtime request for Momentum and Cross Section Measurements:

1 day to set up the detector system for the momentum measurements.

3 days to perform pilot measurements:

Tracked primary beam

^{238}U--> ^{237}U, ^{237}Pa (removal measurements)
^{238}U--> ^{238}Np, ^{238}Pa (Delta resonance, new reaction aspects [43])

Fragments
^{233}U--> ^{232}U, ^{232}Pa (removal measurements)

^{229}U--> ^{228}U, ^{228}Pa (removal measurements)

In total we request for this pioneering run 4 days.

References

[1] M. Bernas et al., Physics Letters B331 (1994) 19.
[2] C. Engelmann et al., Z. Phys. A352 (1995) 351.
[3] P. Armbruster et al., Phys. Rev. Lett. 93 (2004) 212701.
[4] Patent Nr. 4410587: P. Armbruster, H. Geissel, G. Münzenberg, M. Bernas Verfahren zur Bestimmung der Transmissionsquerschnitte von Aktiniden für die Transmutation langlebiger Aktinide durch Spallation. März 1996.
[5] H. Geissel et al., Nucl. Instr. Meth. B 204 (2003) 71.
[6] John J. Cowan, Friedrich Karl Thielemann, Physics Today (October 2004) 47.
[7] John J. Cowan, Christopher Sneden, Nature 440 (2006) 1151.
[8] K. Otsuki, G. J. Mathews, T. Kajino, New Astronomy 8 (2003) 767.
[9] P. Möller, B Pfeiffer and K.-L. Kratz, Phys. Rev. C 67 (2003) 055802.
[10] H. V. Klapdor, J. Metzinger and T. Oda, At. Data and Nucl. Data Tables 31 (1984) 81.
[11] Zs. Podolyak, et al. Proposal G-PAC at GSI 'Along the N=126 shell'
[12] C. Scheidenberger, et al. Phys. Rev. Lett. 77 (1996) 3987.
[13] H. Weick et al., Phys. Rev. Lett. 85 (2000) 2725.
[14] I. Tanihata, et al., Phys. Rev. Lett. 55 (1985) 2676.
[15] T. Suzuki et al., Nucl. Phys. A616, (1997) 286.
[16] A. Ozawa, et al., Nucl. Phys. A608, (1996), 63.
[17] L. Chulkov, et al., Nucl. Phys. A 674 (200) 330.
[18] J. Meng, et al., Phys. Lett. B 419, (1998) 1.
[19] L.Chen, PhD thesis University of Giessen 2008.
[20] K. Sümmerer and B. Blank, Phys. Rev. C 61, 034607 (2000).
[21] J.-J. Gaimard and K.-H. Schmidt, Nucl. Phys. A531, 709 (1991).
[22] J. Benlliure et al., Nucl. Phys. A 660 (1999) 87.
[23] Iwasa et al., Nucl. Instrum. Meth. B 126, 284 (1997)
[24] O.Tarasov and D.Bazin, NIM B 204 (2003) 174.
[25] T. Kurtukian-Nieto, J. Benlliure, et al., arXiv nucl-ex 0711.0101v1, sub. Phys. Lett. B.
[26] H. V. Klapdor, J. Metzinger, and T. Oda, At. Data Nucl. Data Tab. 31 (1984) 81-111.
[27] P. Möller, B. Pfeiffer, K.-L. Kratz, Phys. Review C 67 (2003) 055802.
[28] T. Kurtukian-Nieto J. Benlliurea, K.-H. Schmidt, Nucl. Instr. Meth. A 589 (2008) 472
[29] R. Hofstadter, Ann. Rev. Nucl. Sci. 7 (1957) 231.

[30] C.J. Batty et al. Phys. Rep. 287 (1997) 385.
[31] E. W. Otten in: Treatise of Heavy Ion Science Vol 8, (1989) 517, Ed. D. A. Bromley.
[32] J. Jastrzebski, et al. Nucl. Phys. A558 (1993) 405c
[33] A. Trzcinska, et al. Nucl. Phys. A692 (2001) 176c.
[34] W. Schwab et al., Z. Phys. A 350, 283 (1995).
[35] D. Cortina et al., European Physical Journal A (2001) vol.10, no.1, p.49-56.
[36] W.H. Long et al., Phys. Rev. C 76, (2007) 034314.
[37] H. Lenske, P. Kienle Physics Letters B 647, 2007,82.
[38] M. Samyn, S. Goriely, J. M. Pearson, Nucl.Phys. A725, (2003) 69
[39] M. Samyn, S. Goriely, P. -H. Heenen, J. M. Pearson and F. Tondeur Nucl. Phys. A700 (2002) 142.
[40] E. Nadjakov, K. Marinova and Y. Gangrsky (1994) At. Data and Nucl. Data Tab. 56, 134.
[41] G. A. Lalazissis, S. Raman and P.Ring, At. Data and Nucl. Data Tab. 71, 1-40 (1999).
[42] H. Geissel et al., Phys.Rev.Lett. 88 (2002) 122301.
[43] A. Kelic et al. , Phys Rev. C 70 (2004) 064608